

Steric and Solvation Effects in Ionic S_N2 Reactions

Xin Chen,[†] Colleen K. Regan,[†] Stephen L. Craig,^{†,||} Elizabeth H. Krenske,[‡]
K. N. Houk,[‡] William L. Jorgensen,[§] and John I. Brauman^{*,†}

Department of Chemistry, Stanford University, Stanford, California 94305-5080, Department of
Chemistry and Biochemistry, University of California, Los Angeles, California 90095-1569,
Department of Chemistry, Yale University, New Haven, Connecticut 06520-8107, and
Department of Chemistry, Duke University, Durham, North Carolina 27708-0354

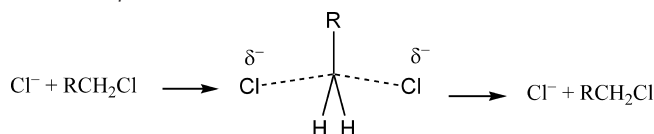
Received June 29, 2009; E-mail: brauman@stanford.edu

Abstract: This paper explores the contribution of solvation to the overall steric effects of S_N2 reactions observed in solution. The reactions of chloride ion with a series of alkyl chloronitriles, RCH(CN)Cl (R = methyl, ethyl, isopropyl, *tert*-butyl) were investigated both experimentally and theoretically. These reactions serve as a model system for the parent reactions, Cl⁻ + RCH₂Cl, which are too slow to measure. Each additional substitution at the β-carbon lowers the reactivity, clearly demonstrating a steric hindrance effect. The magnitude of the steric effect, however, is not significantly different in the gas phase and in solution. We conclude that the solvation energies of the corresponding S_N2 transition states must be similar regardless of size of the substituent. This lack of size dependence in the current system is in sharp contrast with many other ionic systems such as ionization of simple alkyl alcohols, where solvation depends strongly on size. We propose that the weak size dependence results from the compensation between a direct shielding effect of the substituent and an indirect ionic solvation effect, which arises from the geometric perturbations introduced by the substitution. The conclusion is further supported by calculations using polarizable continuum models and QM/MM simulations.

Introduction

The steric effect is an important concept in organic chemistry. A textbook example is the retardation of S_N2 reactivity by bulky alkyl substitution.^{1–6} The chloride exchange reaction in Scheme 1 proceeds more slowly with each additional methyl groups at the β-position. These reactions form the β-series, including methyl, ethyl, isopropyl, and *tert*-butyl substitutions.^{7,8} The steric effect can be defined as the difference in the activation barriers between a sterically hindered reaction and a model, less hindered one. It is often attributed to the repulsive nonbonding interactions between the bulky R group and the nucleophile and/or the

Scheme 1. β-Series of the S_N2 Transition States^a



^a R = methyl, ethyl, isopropyl, *tert*-butyl.

leaving group. The experimentally measured steric effects in solutions, however, are results of combinations of many factors, as long as they are different in the transition states (relative to their respective reactants). An in-depth understanding requires that all of these factors, particularly solvation effects, be taken into consideration.

The effects of structure and solvation are inextricably linked in solution chemistry. This is particularly important for reactions involving ionic species because of their high solvation energy, typically 50–100 kcal mol⁻¹, which is comparable to that of a conventional covalent bond. Differential solvation effects are sometimes large enough to mask differences in intrinsic properties for ionic species. A striking example is the acidities of simple aliphatic alcohols: smaller alcohols are less acidic than larger ones in the gas phase, whereas in solution the order is just the opposite.⁹ The solvation of small alkoxides is sufficiently favorable that it overcompensates the intrinsic difference in acidities, resulting in the reversed order in solution. It is now well-known that barriers to S_N2 reactions in solution

[†] Stanford University.

^{||} Duke University.

[‡] University of California, Los Angeles.

[§] Yale University.

- (1) *Steric Effects in Organic Chemistry*; Newman, M. S., Ed.; John Wiley and Sons: New York, 1956.
- (2) Ingold, C. K. *Structure and Mechanism in Organic Chemistry*, 2nd ed.; Cornell University Press: Ithaca, 1969.
- (3) Lowry, T. H.; Richardson, K. S. *Mechanism and Theory in Organic Chemistry*; Harper Collins: New York, 1987.
- (4) Reichardt, C. *Solvents and Solvent Effects in Organic Chemistry*; VCH: New York, 1988.
- (5) DeTar, D. F.; McMullen, D. F.; Luthra, N. P. *J. Am. Chem. Soc.* **1978**, *100*, 2484–2493.
- (6) Anslyn, E. V.; Dougherty, D. A. *Modern Physical Organic Chemistry*; University Science Books: Sausalito, CA, 2006.
- (7) They may also be called ethyl, *n*-propyl, *iso*-butyl, *neo*-pentyl groups if the center carbon is also counted.
- (8) Some literature also includes the unsubstituted parent reaction, Cl⁻ + CH₃Cl, into this series. However, this is less appropriate because the difference between the parent reaction and methyl substituted one is an α-methyl group while the difference between the rest of the series is a β-methyl group.

(9) Brauman, J. I.; Blair, L. K. *J. Am. Chem. Soc.* **1970**, *92*, 5986–5992.

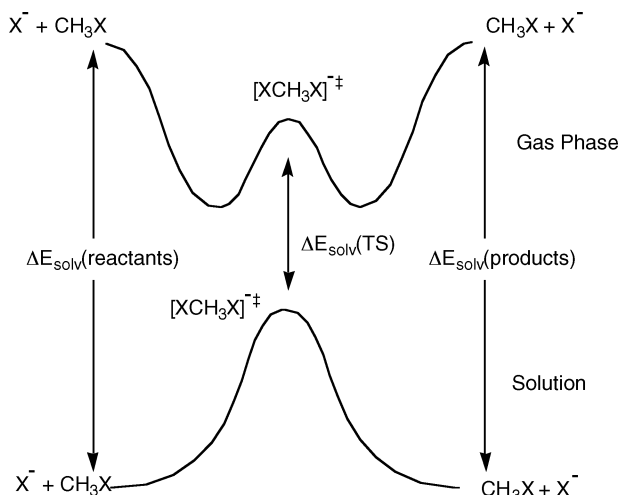


Figure 1. Comparison of gas-phase and solution-phase S_N2 potential energy surfaces.

are largely due to desolvation.^{4,10–14} The smaller ionic nucleophile (X⁻) is solvated much better than the transition state, which is a large and dispersed ion, Figure 1. This raises the question of whether the barriers in solution are affected as much by solvation as by structure. If we assume that a sterically encumbered transition state, which is also much larger in size, is solvated differently compared to a smaller transition state, the steric effect in solution would contain contributions from solvation, as proposed in our previous study.¹⁵ However, recent theoretical work suggests little contribution from solvation to the steric effect, at least between methyl and *tert*-butyl substitution.¹⁶

The question how solvation affects steric effects could be directly answered by comparing the steric effects of the same system in solution and in the gas phase. In practice, however, it is difficult to find a series of S_N2 reactions convenient to work with in both phases. Gas-phase S_N2 reactions between various nucleophiles and alkyl chloride and alkyl bromide have been systematically studied by DePuy and co-workers.¹⁷ However, most of the sterically hindered reactions are too slow to measure accurately, or their corresponding unhindered reactions are too fast. Many of them are further complicated by competing reactions and/or high exothermicity. E2 reactions, which typically generate the same ionic product in the gas phase (and therefore are not directly distinguishable in mass spectrometry), are often faster than the competing S_N2 reaction.^{17–19} The possibility of an E2 reaction can be eliminated in reactions of chloride ion with alkyl bromides because it is thermodynamically

less favorable.^{17,20–24} However, S_N2 reactions between these reactants are exothermic in the gas phase, whereas they are nearly thermoneutral in solution. As discussed by Marcus and other researchers,^{25,26} exothermic reactions have a barrier-lowering effect, which could mask a structural effect, making the interpretation much more difficult.

We chose to study the thermoneutral chloride exchange S_N2 reactions of alkyl chloronitriles. Cyano substitution on methyl chloride dramatically accelerates the S_N2 reactivity compared with the unsubstituted reaction.^{17,27} In addition, these cyano-substituted systems are believed to exhibit statistical behavior, unlike the analogous alkyl halide systems, allowing for modeling with statistical theories.²⁸ In this work, we extend our previous experimental study¹⁵ to the whole β -series of chloronitriles, Cl⁻ + RCH(CN)Cl, as model systems for the Cl⁻ + RCH₂Cl reactions. Comparison between the experimental results and those in solution shows that the magnitude of steric hindrance is similar in the two phases, and we conclude that overall solvation contributes little to the steric hindrance in solution in this β -series. This result is consistent with an earlier analysis that focused on methyl versus *tert*-butyl substitution.¹⁶ To further explore why the solvation differences are so small, quantum calculations were performed for both gas-phase and solution-phase reactions, the latter with a conductor polarizable continuum model (CPCM)^{29,30} and an isodensity polarizable continuum model (IPCM).³¹ The calculations and our analysis suggest that the lack of net contribution from solvation in this particular system is a result of the compensation between a negative solvent shielding effect and a positive ionic solvation effect. While our paper was in preparation, Truhlar and co-workers submitted work applying a different theoretical method^{32,33} to the same question. Our results are consistent with theirs.³⁴

Experimental Section

Instrument. The experiments were carried out using an IonSpec OMEGA Fourier transform ion cyclotron resonance spectrometer (FT-ICR), which has been described previously.³⁵ The magnetic field strength was 0.6 T. The temperature of the 2 in. cubic stainless

- (10) Olmstead, W. N.; Brauman, J. I. *J. Am. Chem. Soc.* **1977**, *99*, 4219–4228.
 (11) Chandrasekhar, J.; Smith, S. F.; Jorgensen, W. L. *J. Am. Chem. Soc.* **1984**, *106*, 3049–3050.
 (12) Chandrasekhar, J.; Smith, S. F.; Jorgensen, W. L. *J. Am. Chem. Soc.* **1985**, *107*, 154–163.
 (13) Chabinye, M. L.; Craig, S. L.; Regan, C. K.; Brauman, J. I. *Science* **1998**, *279*, 1882–1886.
 (14) Viggiano, A. A.; Paschkewitz, J. S.; Morris, R. A.; Paulson, J. F.; Gonzalezlafont, A.; Truhlar, D. G. *J. Am. Chem. Soc.* **1991**, *113*, 9404–9405.
 (15) Regan, C.; Craig, S.; Brauman, J. *Science* **2002**, *295*, 2245–2247.
 (16) Vayner, G.; Houk, K.; Jorgensen, W.; Brauman, J. *J. Am. Chem. Soc.* **2004**, *126*, 9054–9058.
 (17) DePuy, C. H.; Gronert, S.; Mullin, A.; Bierbaum, V. M. *J. Am. Chem. Soc.* **1990**, *112*, 8650–8655.
 (18) Gronert, S. *Acc. Chem. Res.* **2003**, *36*, 848–857.
 (19) Hu, W. P.; Truhlar, D. G. *J. Am. Chem. Soc.* **1996**, *118*, 860–869.

- (20) Caldwell, G.; Magnera, T. F.; Kebarle, P. *J. Am. Chem. Soc.* **1984**, *106*, 959–966.
 (21) van der Wel, H.; Nibbering, N. M. M.; Sheldon, J. C.; Hayes, R. N.; Bowie, J. H. *J. Am. Chem. Soc.* **1987**, *109*, 5823–5828.
 (22) Knighton, W. B.; Bogner, J. A.; O'Connor, P. M.; Grimsrud, E. P. *J. Am. Chem. Soc.* **1993**, *115*, 12079–12084.
 (23) Li, C.; Ross, P.; Szulejko, J. E.; McMahon, T. B. *J. Am. Chem. Soc.* **1996**, *118*, 9360–9367.
 (24) Sahlstrom, K. E.; Knighton, W. B.; Grimsrud, E. P. *J. Phys. Chem. A* **1997**, *101*, 1501–1508.
 (25) Marcus, R. A. *Annu. Rev. Phys. Chem.* **1964**, *15*, 155–196.
 (26) Wladkowski, B. D.; Brauman, J. I. *J. Phys. Chem.* **1993**, *97*, 13158–13164.
 (27) Wladkowski, B. D.; Lim, K. F.; Allen, W. D.; Brauman, J. I. *J. Am. Chem. Soc.* **1992**, *114*, 9136–9153.
 (28) Viggiano, A. A.; Morris, R. A.; Su, T.; Wladkowski, B. D.; Craig, S. L.; Zhong, M.; Brauman, J. I. *J. Am. Chem. Soc.* **1994**, *116*, 2213–2214.
 (29) Barone, V.; Cossi, M. *J. Phys. Chem. A* **1998**, *102*, 1995–2001.
 (30) Barone, V.; Cossi, M.; Tomasi, J. *J. Comput. Chem.* **1998**, *19*, 404–417.
 (31) Foresman, J. B.; Keith, T. A.; Wiberg, K. B.; Snoonian, J.; Frisch, M. J. *J. Phys. Chem. A* **1996**, *100*, 16098–16104.
 (32) Hawkins, G. D.; Cramer, C. J.; Truhlar, D. G. *Chem. Phys. Lett.* **1995**, *246*, 122–129.
 (33) Zhao, Y.; Truhlar, D. G. *Acc. Chem. Res.* **2008**, *41*, 157–167.
 (34) Kim, Y.; Cramer, C. J.; Truhlar, D. G. *J. Phys. Chem. A* **2009**, *113*, 9109–9114.
 (35) Zhong, M.; Brauman, J. I. *J. Am. Chem. Soc.* **1996**, *118*, 636–641.

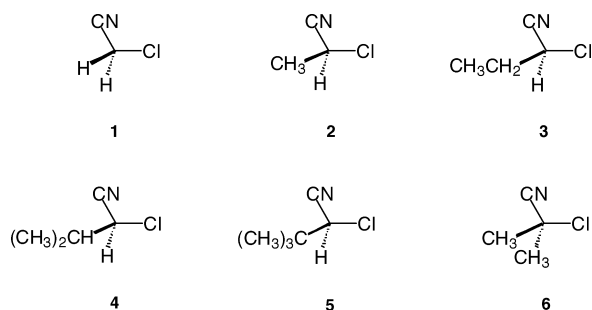


Figure 2. Alkyl-substituted chloronitriles.

steel cell was estimated to be 350 K.³⁶ Background pressures were $1.0\text{--}4.0 \times 10^{-9}$ Torr, and operating pressures were $0.3\text{--}2.4 \times 10^{-6}$ Torr. A Granville Phillips 330 ion gauge was used to obtain pressure readings, which were calibrated against a MKS Baratron 170 capacitance manometer (315BH-1 sensor). Absolute pressure measurements were estimated to have an error of $\pm 20\%$ due to the calibration of the ion gauge with the capacitance manometer. The difficulty in measuring absolute pressures of compounds of low volatility also contributed to the error.

Materials. The chloronitriles include chloroacetonitrile, **1**; 2-chloropropionitrile, **2**; 2-chloro-*n*-butyronitrile, **3**; 2-chloroisobutyronitrile, **4**; 2-chloro-3,3-dimethylbutyronitrile, **5**; and 2-chloroisobutyronitrile, **6**, as shown in Figure 2. Among the reagents not commercially available, **6** was synthesized directly from isobutyronitrile,³⁷ and **3**, **4**, and **5** were synthesized according to literature procedures, by first converting the corresponding aldehydes to cyanohydrins³⁸ and then to the target chloronitriles.³⁹ The chloronitriles **2**, **3**, **4**, and **5**, RCH(CN)Cl (R = methyl, ethyl, isopropyl, *tert*-butyl), form a complete β -series and serve as good comparisons to RCH₂Cl. All of the chloronitriles were extensively purified by low-pressure distillation and by preparatory gas chromatography. No contaminant ion peaks were observed in either the ¹H NMR or positive ion mass spectra. Multiple unique samples of each chloronitrile were used in experiments and had results with close agreement. All compounds were subject to multiple freeze-pump-thaw cycles before use.

Chloride Binding Equilibria. Chloride ion complexation energies were determined from chloride exchange equilibrium between the chloronitriles and reference compounds, eq 1. The complex ions were generated by the method of Larson and McMahon.^{40,41}



Equilibrium constants, K_{eq} , eq 1, were determined by monitoring the ratio of complexes over time. Equilibrium was generally reached within 1200 ms under typical experimental conditions. To ensure

that a true equilibrium was reached, all but one complex was ejected, and the equilibrium was allowed to be reestablished. This complex was monitored over time against the appearance of one or more competing complexes until a steady ratio was reached. The equilibrium ratio was independent of the complex initially retained. Relative free energies of chloride binding can be obtained from equilibrium ratios, $\Delta G_{\text{rel}}^\circ = -RT \ln K_{\text{eq}}$. Absolute values were determined by bracketing $\Delta G_{\text{rel}}^\circ$ of the chloronitrile compounds against known $\Delta G_{\text{abs}}^\circ$ values for the reference compounds. Experiments carried out on multiple days and at multiple pressure ratios with various combinations of neutral compounds demonstrate high reproducibility of $<10\%$. Each equilibrium measurement reported in this study is the average of at least six trials. Error in experimental absolute equilibrium constants is assigned at 20% due to error in absolute pressure measurements.

Kinetics. Rate constants of these identity exchange reactions were measured by isotope exchange of chloride. Chloride ion was generated by electron impact ionization on the chloronitrile. Primary ion formation lasted for 20 ms. Free electrons were then ejected for 40 ms. The natural abundance ratio of 3:1 for ³⁵Cl⁻ to ³⁷Cl⁻ was obtained before each kinetic run. After ion thermalization, the less abundant ³⁷Cl⁻ isotope was then isolated and allowed to react with the neutral chloronitrile over a period of up to 4500 ms. The ion intensities of ³⁷Cl⁻ and ³⁵Cl⁻ were monitored as a function of time as the equilibrium ratio was reestablished. The rate of appearance of ³⁵Cl⁻ was corrected for the natural isotopic abundance ratio and then converted into a rate constant using the method of Eyler and Richardson.⁴² Ratios of ion abundances instead of absolute ion signals are analyzed as a function of time. This method eliminates errors from ion loss, as long as rates of ion loss are nearly equal for reactant and product ions, a good assumption for identity exchange reactions.²⁷ Good first order kinetics were always observed for the reactions across a pressure range of 5×10^{-7} to 2.5×10^{-6} Torr. Rate constants were pressure-independent and were reproducible to within $\pm 5\%$ across the pressure range. Absolute errors in the rate constants are ascribed almost entirely to difficulty in determining absolute pressures and are taken to be $\pm 30\%$. The error in absolute pressure measurements is likely to be systematic, so the uncertainty in the relative rate constants is smaller, $\pm 10\%$. The central S_N2 barrier, ΔE_{diff} , is determined from fitting the experimental reaction efficiencies with Rice–Ramsperger–Kassel–Marcus (RRKM) unimolecular reaction rate theory.^{27,43} The reaction efficiency, Φ , is defined as the competition between decomposition of the ion molecule complex back to reactants and passage over the S_N2 barrier toward a second ion molecule complex and is determined by dividing the experimental rate constant by the collision capture rate constant. Capture rates were determined through use of a parametrized trajectory model by Su and Chesnavich.⁴⁴

Calculations. The S_N2 reactions of chloride with the alkyl-substituted chloronitrile series were calculated with a complete basis set theory CBS-QB3.⁴⁵ The results were compared with the alkyl chloride series. Two polarizable continuum models, IPCM and CPCM, were used to calculate the solvation energies at B3LYP/6-311+(2d,p) level of theory^{29–31} with geometries optimized in the gas phase using the same level of theory. In another set of calculations, activation energies (ΔG^\ddagger) in solution were calculated by adding to the CBS-QB3 values a free energy of solvation, which was obtained by optimization of the relevant geometries in solution at the B3LYP/6-31G(d) level using the CPCM-UAKS model. In

(36) Han, C. C.; Brauman, J. I. *J. Am. Chem. Soc.* **1989**, *111*, 6491–6496.

(37) Stevens, C. L. *J. Am. Chem. Soc.* **1948**, *70*, 165–166.

(38) Davis, J. W. *J. Org. Chem.* **1978**, *43*, 3980–3982.

(39) Carman, R. M.; Shaw, I. M. *Aust. J. Chem.* **1976**, *29*, 133–143.

(40) Larson, J. W.; McMahon, T. B. *J. Am. Chem. Soc.* **1984**, *106*, 517–521.

(41) Larson, J. W.; McMahon, T. B. *J. Am. Chem. Soc.* **1985**, *107*, 766–773.

(42) Eyler, J. R.; Richardson, D. E. *J. Am. Chem. Soc.* **1985**, *107*, 6130–6131.

(43) Gilbert, R. G.; Smith, S. C. *Theory of Unimolecular and Recombination Reactions*; Blackwell Scientific: Oxford, 1990.

(44) Su, T.; Chesnavich, W. J. *J. Chem. Phys.* **1982**, *76*, 5183–5185.

(45) Montgomery, J. A.; Frisch, M. J.; Ochterski, J. W.; Petersson, G. A. *J. Chem. Phys.* **1999**, *110*, 2822–2827.

Table 1. Complexation Energies of Cl^- with Chloronitriles (kcal mol^{-1})

chloronitrile	$\Delta G^\circ_{\text{exp}}$	$\Delta H^\circ_{\text{exp}}$	ΔH_{DFT}
1	-13.1	-19.3	-18.2
2	-13.2	-19.4	-18.2
3	-12.7	-18.9	-18.4
4	-13.4	-19.6	-18.4
5	-13.0	-19.2	-18.6
6	-10.9	-17.1	-15.6

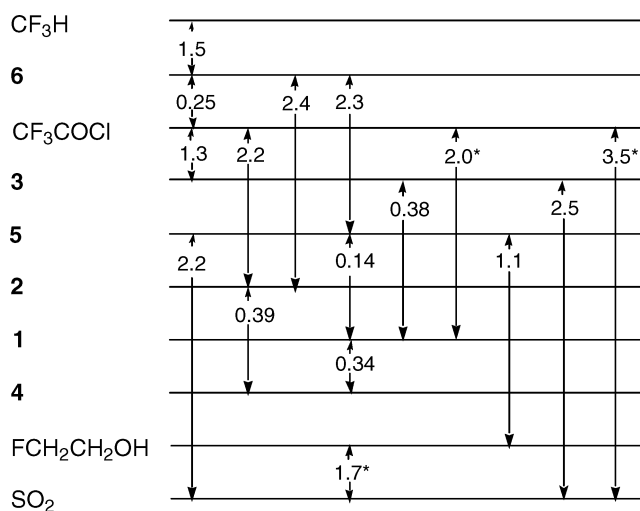
contrast to earlier work,¹⁶ the UAKS cavity was chosen here because there is evidence that it performs better than UAHF or UA0.⁴⁶

QM/MM calculations with explicit representation of the water molecules in aqueous solution on the structures of S_N2 transition states were also carried out. The approach features the semiempirical QM method, PDDG/PM3, in conjunction with free-energy perturbation (FEP) calculations in Metropolis Monte Carlo (MC) simulations; all calculations were performed with the BOSS program.⁴⁷ Briefly, the MC simulations modeled the reactants and 740 water molecules in a periodic box using the isothermal isobaric (NPT) ensemble at 25 °C and 1 atm. The water was represented with the TIP4P potential energy function,⁴⁸ and the energetics of the reacting system are described by PDDG/PM3.^{49,50} The solute–water interactions consist of Lennard-Jones terms, described with OPLS-AA parameters,⁴⁸ and Coulomb terms using the TIP4P atomic charges for water and solute charges computed with the CM3P method.^{51,52} The MC/FEP calculations allow determination of free-energy changes for variation of the solute's geometry. To locate the S_N2 transition structures in water, it was previously found that the two C–Cl distances were essentially identical, so the free energy was mapped as a function of the C–Cl distance and Cl–C–Cl angle with all other degrees of freedom sampled.¹⁶ The increment between FEP calculations (windows) was 0.01 Å and 1.0°. Upon each attempted MC move of the solutes, a PDDG/PM3 single-point calculation was performed for the reference and perturbed solutes. Each FEP window covered 2.5 million MC configurations of equilibration, followed by 5 million configurations of averaging with an attempted move of the solute every 100 configurations. The water–water interactions were truncated and smoothed at O–O separations of 10 Å, and water–solute interactions were included if any O–C or O–Cl distance was less than 10 Å.

Results

Potential Energy Surface. Table 1 lists the chloride ion complexation energies, determined from chloride exchange equilibria, Figure 3. Equilibrium constants measured for chloride binding of these compounds were converted into relative free energies, $\Delta G^\circ = -RT \ln K_{\text{eq}}$. Conversion to ΔH° involved determination of ΔS° , the values of which were taken to be identical to the previously determined entropy for complexation of **1** with chloride ion (17.7 cal $\text{mol}^{-1} \text{K}^{-1}$)²⁴ with correction for symmetry when necessary.

The experimentally determined complexation enthalpies were ~ 19 kcal mol^{-1} , slightly greater than typical ion–molecule

**Figure 3.** Ladder of relative ΔG° (kcal mol^{-1}) for chloride ion equilibrium exchange reactions. Numbers correspond to chloronitriles from Figure 2. Starred values are from refs 35 and 36.**Table 2.** Experimental Kinetics and Energetics for Reactions of Cl^- with Chloronitriles

	RCH(CN)Cl	k_{exp}^a	Φ	ΔE_{diff}^b
2	methyl	1.0×10^{-11}	0.003	-1.6
3	ethyl	8.9×10^{-12}	0.003	-1.8
4	isopropyl	2.7×10^{-12}	0.001	-0.6
5	<i>tert</i> -butyl	1.1×10^{-12}	0.0004	0.3

^a Units are $\text{molecules}^{-1} \text{s}^{-1} \text{cm}^3$. ^b Units are kcal mol^{-1} .

complexes in the gas phase (~ 15 kcal mol^{-1}). The values were almost the same except for **6**, which was ~ 2 kcal mol^{-1} less stable than those for **1–5**. The ion complexation was generally electrostatic in origin, but in this system, we believe that hydrogen bonding also contributes a modest amount. All of the chloronitriles have almost the same dipole moments, and ion–dipole interactions should be similar. On the other hand, all compounds except **6** have an acidic α -hydrogen, which explains its lower complexation energy. This is not a typical ionic hydrogen bond, and its strength is much weaker, only about 2 kcal mol^{-1} . The results were supported by DFT calculations at the B3LYP/6-31+G* level, which showed hydrogen bonding for all the complexes except **6**. The absolute values of the complexation energies were underestimated by DFT calculations, which often biases toward more dispersed charge,³³ but the errors appear to be systematic and the relative errors are much smaller (Table 1).

Kinetic rates measured from chloride isotope exchange reactions for β -substituted compounds are listed in Table 2. Rates were reproducible to 10% across the pressure range studied. Great effort was taken to minimize error, especially for slow reactions. To obtain the barrier heights of the transition states, the rate constants were first converted into reaction efficiencies, Φ , in Table 2. The central barriers were then determined by fitting the reaction efficiencies with RRKM theory.^{27,43} The barrier heights relative to the reactants, ΔE_{diff} , are reported in Table 2. The data show an increase of the barrier height with larger alkyl groups, except from methyl to ethyl, where a slight decrease was observed. This phenomenon has been previously observed in studies of chloride ion with

- (46) Takano, Y.; Houk, K. N. *J. Chem. Theory Comput.* **2005**, *1*, 70–77.
 (47) Jorgensen, W. L.; Tirado-Rives, J. *J. Comput. Chem.* **2005**, *26*, 1689–1700.
 (48) Jorgensen, W. L.; Tirado-Rives, J. *Proc. Natl. Acad. Sci. U.S.A.* **2005**, *102*, 6665–6670.
 (49) Repasky, M. P.; Chandrasekhar, J.; Jorgensen, W. L. *J. Comput. Chem.* **2002**, *23*, 1601–1622.
 (50) Tubert-Brohman, I.; Guimaraes, C. R. W.; Repasky, M. P.; Jorgensen, W. L. *J. Comput. Chem.* **2004**, *25*, 138–150.
 (51) Thompson, J. D.; Cramer, C. J.; Truhlar, D. G. *J. Comput. Chem.* **2003**, *24*, 1291–1304.
 (52) Udier-Blagovic, M.; De Tirado, P. M.; Pearlman, S. A.; Jorgensen, W. L. *J. Comput. Chem.* **2004**, *25*, 1322–1332.

Table 3. Energetics (CBS-QB3, kcal mol⁻¹) and Geometries (B3LYP/CBSB7) of Transition States of Cl⁻ with Alkyl Chlorides and Chloronitriles

	RCH ₂ Cl			RCH(CN)Cl		
	ΔE_{diff}	$r(\text{C}-\text{Cl})^a$	$\angle(\text{Cl}-\text{C}-\text{Cl})$	ΔE_{diff}	$r(\text{C}-\text{Cl})^a$	$\angle(\text{Cl}-\text{C}-\text{Cl})$
methyl	4.5	2.436 Å	163°	-0.7	2.454 Å	160°
ethyl	3.2	2.441 Å	163°	-1.8	2.460 Å	160°
isopropyl	4.8	2.462 Å	158°	0.3	2.484 Å	155°
<i>tert</i> -butyl	10.3	2.508 Å	147°	5.7	2.540 Å	143°

^a Some of the transition states are not symmetrical, and for those the bond distances are the average of the two.

analogous alkyl bromides and attributed to the polarization effect of the extra methyl group.^{17,23,53,54}

To compare with the experimental results, quantum calculations were performed using CBS-QB3 model. The parent reactions of Cl⁻ + RCH₂Cl were also calculated with the same theory. The values for methyl and *tert*-butyl substitution calculated at the same theory have been previously reported in an independent study.¹⁶ The activation energy ΔE_{diff} and the key parameters of the geometries are listed in Table 3. CBS-QB3 estimates the barrier to within 1 kcal mol⁻¹ of the experimental barrier for methyl, ethyl, and isopropyl but is off by more than 4 kcal mol⁻¹ for *tert*-butyl. The methyl and *tert*-butyl results reproduced the previous calculations.¹⁶ Similar results were obtained in a recently submitted theoretical study.³⁴ The significant disagreement between the experiment and the theory for *tert*-butyl suggests that the measured experimental rate for *tert*-butyl was actually higher than the true value because of a reactive contaminant, even though no such indication was found in repeated experiments. Contamination at the level of 4×10^{-4} would account for the problem. Although we do not understand the exact source of the discrepancy, we believe that the problem lies with the experiment rather than the theory.

The RCH(CN)Cl (R = methyl, ethyl, isopropyl, *tert*-butyl) chloronitriles form a complete β -series and can be compared to RCH₂Cl. The S_N2 reactions of Cl⁻ + RCH₂Cl have been widely investigated before with many methods such as AM1, HF and MP2, and CBS-QB3.^{55,56,16,57} The predicted transition state geometries are similar for most methods. Larger substituents always result in longer C–Cl bond lengths. According to CBS-QB3 (geometry optimized with B3LYP/CBSB7), the bonds are stretched 0.02–0.04 Å with each additional methyl group. The Cl–C–Cl bond angle decreases gradually, from 163° in methyl to 147° in *tert*-butyl. The corresponding geometries in the RCH(CN)Cl are slightly more extended and more distorted than in the parent systems. For example, the Cl–C–Cl angle is about 3–4° smaller, and the C–Cl bond lengths are 0.02–0.03 Å longer. Energetically, CBS-QB3 predicts that the cyano substitution consistently lowers the barrier by ~5 kcal mol⁻¹ relative to the unsubstituted reactions. It appears that α -cyano substitution does not perturb the β -positions significantly. Both energetic and geometric differences between the two systems are almost constant throughout the whole series, indicating that the chloronitriles are good model systems for alkyl chlorides.

Table 4. IPCM and CPCM Solvation Energies of S_N2 Transition States, Alkoxides, and Carboxylates (kcal mol⁻¹) in Water

R	IPCM			CPCM		
	Cl–RCH ₂ –Cl ⁻	RO ⁻	RCOO ⁻	Cl–RCH ₂ –Cl ⁻	RO ⁻	RCOO ⁻
methyl	-54.9	-72.1	-67.7	-55.8	-71.4	-68.7
ethyl	-54.3	-69.3	-67.5	-55.3	-69.4	-67.3
isopropyl	-54.3	-67.1	-67.2	-55.0	-66.1	-66.2
<i>tert</i> -butyl	-55.0	-63.8	-65.8	-54.7	-63.2	-63.5

PCM Calculations of Solvation Energy. To directly evaluate the solvation contribution to the steric effect, the solvation energies of the Cl–R–Cl⁻ transition states were estimated with two polarizable continuum models, IPCM and CPCM. Both of them have been used previously to investigate the steric effect.^{16,58} These two models showed no qualitative difference in our systems.

The solvation energies of the S_N2 transition states were estimated to be 50–60 kcal mol⁻¹, which was much smaller than that of the nucleophile Cl⁻ (69 and 76 kcal mol⁻¹ predicted by IPCM and CPCM respectively). The difference in solvation energy between the reactants and the transition state results in the increased activation energy in solution, Figure 1. However, no significant difference can be observed, when one compares the solvation energies of different transition states in the β -series, despite their different sizes. Both IPCM and CPCM predicts virtually no difference along the β -series, Table 4.

The lack of size dependence in these transition states is surprising when compared with alkoxides and carboxylates with the same substitution groups. The solvation energies of these substituted alkoxides and carboxylates were also calculated with the same method, and the results are also shown in Table 4 for comparison. Interestingly, both alkoxides and carboxylates demonstrate the clear trend of negative size dependence, according to both IPCM and CPCM. The stark contrast to the β -series of the S_N2 transition states (Cl–RCH₂–Cl⁻) suggests that solvation of the transition states is fundamentally different from that of simple stable ions.

We hypothesize that geometrical changes in the transition states are responsible for the different size dependencies of solvation observed among the above systems. Additional methyl groups near the reaction center can significantly perturb the transition state geometry (Table 3).^{16,55,56} To investigate the relationship between the geometry and the solvation in these transition states, a set of calculations was conducted with the fixed geometries at the reaction center for the whole β -series. The relative positions among the three atoms, the two chlorides and the central carbon, were frozen during the optimization. The partially frozen transition states were calculated with CPCM and IPCM to evaluate their solvation energies. For example, the CPCM solvation energy of the methyl transition state with the *tert*-butyl geometry (C–Cl bond length, Cl–C–Cl angle) was calculated to be -57.4 kcal mol⁻¹, listed as methyl(*tert*-butyl) at the most top-right entry in Table 5. With four substitutions and four configurations, a 4 × 4 table was obtained. From Table 5, one can see that the top-right entries are generally greater (more negative) than bottom-left. The trend will be discussed later. Solvation energies calculated with IPCM and/or in other solvents show similar trends (Supporting Information). The NPA atomic charges on the chlorides are reported in a similar manner, Table 6.

(53) Gronert, S. *Chem. Rev.* **2001**, *101*, 329–360.

(54) Ren, Y.; Yamataka, H. *J. Org. Chem.* **2007**, *72*, 5660–5667.

(55) Jensen, F. *Chem. Phys. Lett.* **1992**, *196*, 368–376.

(56) Anh, N.; Maurel, F.; Thanh, B.; Thao, H.; Nguessan, Y. *New J. Chem.* **1994**, *18*, 473–481.

(57) Fernandez, I.; Frenking, G.; Uggerud, E. *Chem.—Eur. J.* **2009**, *15*, 2166–2175.

(58) Costentin, C.; Saveant, J. M. *J. Am. Chem. Soc.* **2000**, *122*, 2329–2338.

Table 5. CPCM Solvation Energies (kcal mol⁻¹) of Transition States of $R_1(R_2)^a$

	(methyl)	(ethyl)	(isopropyl)	(<i>tert</i> -butyl)
methyl	-55.8	-55.8	-56.2	-57.4
ethyl	-55.3	-55.3	-55.8	-57.1
isopropyl	-54.6	-55.9	-55.0	-56.6
<i>tert</i> -butyl	-52.9	-52.9	-55.1	-54.7

^a R_1 is the substituent and R_2 represents the geometry at which the transition state is calculated. Only the diagonal entries, where $R_1 = R_2$, represent "real" transition states.

Table 6. NPA Charges on Chlorides (Average of the Two) of Transition States of $R_1(R_2)$ in the Gas Phase

	(methyl)	(ethyl)	(isopropyl)	(<i>tert</i> -butyl)
methyl	0.651	0.653	0.659	0.670
ethyl	0.652	0.653	0.660	0.675
isopropyl	0.650	0.663	0.657	0.672
<i>tert</i> -butyl	0.635	0.635	0.669	0.662

Table 7. Free Energies of Activation for S_N2 Reactions in the Gas Phase and in Solution^a

reaction	ΔG^\ddagger			
	gas phase 1 atm	gas phase 1 mol L ⁻¹	acetone 1 mol L ⁻¹	water 1 mol L ⁻¹
MeCH ₂ Cl + Cl ⁻	10.1	12.0	36.3	39.1
EtCH ₂ Cl + Cl ⁻	9.8	11.7	36.8	39.6
ⁱ PrCH ₂ Cl + Cl ⁻	11.7	13.6	38.9	41.7
^t BuCH ₂ Cl + Cl ⁻	17.3	19.2	44.4	46.8
MeCH(CN)Cl + Cl ⁻	6.3	8.2	35.9	39.4
EtCH(CN)Cl + Cl ⁻	5.4	7.3	35.3	39.8
ⁱ PrCH(CN)Cl + Cl ⁻	7.6	9.5	37.2	41.7
^t BuCH(CN)Cl + Cl ⁻	12.6	14.5	42.2	46.7

^a Gas-phase free energies obtained at the CBS-QB3 level and reported as calculated (a) for a standard state of 1 atm and (b) corrected to 1 mol L⁻¹. Solution values obtained by adding the CPCM free energies of solvation for the solution-optimized geometries [optimization and solvation calculation both at the B3LYP/6-31G(d) level] to the corresponding CBS-QB3 gas-phase free energies at 1 mol L⁻¹. All values in kcal mol⁻¹.

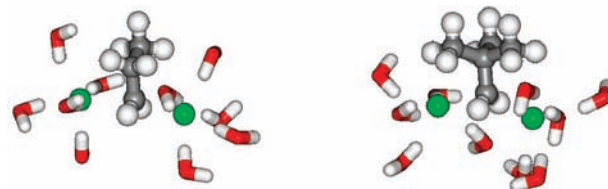
The above calculations are carried out with geometries optimized in the gas phase. In another set of CPCM calculations, we determined solvation energies using geometries optimized in solution at the B3LYP/6-31G(d) level for the parent reactions as well as the cyano-substituted ones (Table 7). The structures optimized in the gas phase with the 6-31G(d) basis set are virtually identical with the CBSB7 basis, used in the CBS-QB3 calculations (Figure S1 and S2 in Supporting Information). Comparison of the gas-phase and solution-optimized B3LYP/6-31G(d) transition structures reveals little difference: the C–Cl bond length is less than a few hundredth angstroms different and the Cl–C–Cl bond angle less than a few degrees (Figures S1 and S2 in Supporting Information). The substituent effects on ΔG^\ddagger , according to these calculations employing solution-optimized geometries (Table 7), are also similar with those in the gas phase (Table 3). For examples of the *tert*-butyl reactions, the substituent effect in solution is only 0–1 kcal mol⁻¹ larger than in the gas phase. Again, these calculations indicate little differential solvation within the β -series.

QM/MM Simulations of S_N2 Transition States. To evaluate the influence of explicit representation of the water molecules in aqueous solution on the structures of S_N2 transition states, QM/MM/MC/FEP calculations were carried out, using the PDDG/PM3 method in conjunction with FEP in MC simulations. The same methodology was used in the earlier study for

Table 8. Transition State Structures and Numbers of Hydrogen-Bonded Water Molecules from PDDG/PM3 optimizations and QM/MM Calculations

	gas phase ^a		water solution ^b		
	$r(\text{C}-\text{Cl})$	$\angle(\text{Cl}-\text{C}-\text{Cl})$	$r(\text{C}-\text{Cl})$	$\angle(\text{Cl}-\text{C}-\text{Cl})$	Cl–H ^c
methyl	2.29 Å	170°	2.30 Å	168°	9.9
ethyl	2.29 Å	169°	2.50 Å	164°	10.0
isopropyl	2.31 Å	163°	2.53 Å	156°	10.0
<i>tert</i> -butyl	2.33 Å	153°	2.54 Å	142°	9.3

^a PDDG/PM3 results. ^b QM/MM/MC/FEP results in TIP4P water at 25 °C and 1 atm. Uncertainties are ± 0.02 Å and $\pm 2^\circ$. ^c Number of TS–water hydrogen bonds, obtained from integrating the Cl–H(water) radial distribution functions. Uncertainty is ± 0.1 .

**Figure 4.** Representative snapshots of the transition states for the reactions of Cl⁻ with propyl and neopentyl chloride in water. The 10 water molecules out of 740 that are hydrogen-bonded to the transition structures are included. From the last configuration in the MC/FEP calculations.

the methyl and *tert*-butyl cases in several solvents with good success.¹⁶ Presently, it was extended to the whole β -series. Key results for the transition structures are summarized in Table 8. In the gas phase, PDDG/PM3 optimizations predict that the C–Cl bond length increases from 2.29 to 2.33 Å and the Cl–C–Cl angle decreases from 170° to 153° in progressing from methyl to *tert*-butyl as the substituent. The results are similar to the DFT findings in Table 3; the bond lengths and angles from PDDG/PM3 are uniformly about 0.15 Å shorter and 5° wider. However, upon progressing to aqueous solution larger changes are predicted from the QM/MM calculations. For methyl through *tert*-butyl, the C–Cl distance increases by 0.2 Å, while the DFT results indicate only ca. 0.02 Å. For the Cl–C–Cl angle, the DFT results predict 2–3° decreases upon transfer to water, while the QM/MM calculations find the decrement to increase from 2° to 10° in progressing from methyl through *tert*-butyl. The changes in the QM/MM results improve the hydration of the chlorines at some distortion expense as the substituent on the electrophilic carbon becomes bulkier. The relatively consistent hydration is reflected in the results for the number of hydrogen-bonded water molecules for the transition states in Table 8. These values are readily obtained from integration of the Cl–H(water) radial distribution functions and water–solute interaction energy distributions, which show clear minima at 2.75 Å and –6.75 kcal/mol, respectively. Illustrations of the transition structures with their hydrogen-bonded water molecules are provided in Figure 4. It may be noted that the free-energy surfaces for the transition structures in water are generally flat to within 0.1 kcal/mol within 0.02 Å and 2° of the listed minima.

Discussion

All chemical and physical properties of molecules observed in solution are subject to solvation. The effect is especially important for ions, the solvation energies of which are often as high as the strength of a typical chemical bond. The differential solvation energy between the ionic species can sometimes mask the intrinsic properties. Here we use acidities as an example.

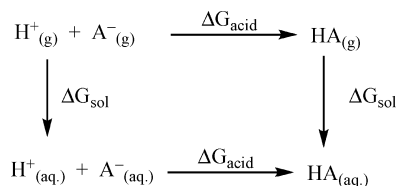


Figure 5. Thermochemical cycle connects the acidity in the gas phase and in water.

The thermochemical cycle in Figure 5 clearly demonstrates that the solution acidities contain contributions from the solvation energies. When comparing two acids, HA₁ and HA₂, the relative acidities in solution, $\Delta\Delta G_{\text{acid,sol}}$, are the summation of the intrinsic values, $\Delta\Delta G_{\text{acid,gp}}$, and the differential solvation, eq 6. Since the solvation energies of neutrals are much smaller than those of ions, their contributions can usually be ignored, eq 7. The solvation energy of the anionic base A[−], however, is much higher and varies significantly among different species. Sometimes, the difference is so large that it reverses the acidity order. For example, methanol is more acidic than ethanol in water, whereas it is just the opposite in the gas phase.⁹ The order is reversed because the smaller alkoxides are solvated more effectively than the larger ones, and the difference in solvation is the dominant factor.

$$\Delta\Delta G_{\text{acid,sol}} = \Delta\Delta G_{\text{acid,g}} + \Delta G_{\text{sol}}(\text{A}_1^-) - \Delta G_{\text{sol}}(\text{A}_2^-) + \Delta G_{\text{sol}}(\text{HA}_2) - \Delta G_{\text{sol}}(\text{HA}_1) \quad (6)$$

$$\Delta\Delta G_{\text{acid,sol}} \approx \Delta\Delta G_{\text{acid,g}} + G_{\text{sol}}(\text{A}_1^-) - \Delta G_{\text{sol}}(\text{A}_2^-) \quad (7)$$

The steric effect in S_N2 reactions would also be affected by solvation in a similar way, as long as the transition states are solvated differently. The goal of this study is to understand the contribution of solvation to the steric hindrance observed in solution. There are two general strategies to attack this problem. The most straightforward method is to compare the steric effects in the gas phase and in solution. Alternatively, one can study the solvation energies of the corresponding transition states directly. Both strategies are adopted in this study, as discussed in the following sections.

Comparing Steric Effects in the Gas Phase and in Solution. We chose the chloronitrile systems, related to alkyl chlorides by substituting a cyano group at the reaction center carbon. Such substitution is known to increase the S_N2 reactivity relative to chloride ion with methyl chloride by several orders of magnitude²⁷ while still keeping the reaction thermoneutral. In addition, the system is believed to behave statistically,²⁸ allowing us to use RRKM theory to determine the barrier height. Similar considerations are expected for larger alkyl groups.

Ab initio calculations do not require consideration of competing reactions and also obviate complicating effects of exothermicity if thermoneutral reactions are studied, even if they are often too slow to measure experimentally. Among the numerous theoretical studies on S_N2 reactions in the literature, a few have focused on steric effects of alkyl substitution.^{5,16,34,55,56,58–62} The parent reactions (Cl[−] + RCH₂Cl) have been investigated

systematically previously with relatively low level methods.^{55,56} We performed CBS-QB3 calculations for the parent reactions as well as for the cyano-substituted systems for comparison. The results show that the cyano-substituted systems resemble the parent reactions very well, both energetically and geometrically. These results are consistent with the previous conclusion based on methyl and *tert*-butyl substitution.¹⁶

Table 9 compares the solution data with the gas-phase barrier heights of our systems, together with our CBS calculation results in the gas phase. Since steric effects are only meaningful as relative terms, the barrier heights listed are relative to methyl. All solution data, compiled by DeTar et al., are taken from ref 5, and the original data can be found in references therein. In solution, the steric effect is not very sensitive to the identity of the halides. Hetero halide exchange reactions demonstrate steric effects similar to those in our identity halide exchanges. One possible reason is that the exothermicities of all listed reactions are very small in solution. Note that the barrier heights reported in solution are enthalpies rather than energies as in the gas phase. The relative difference is small.

In most systems listed in Table 9, ethyl shows a barrier height similar to that of methyl, and isopropyl's is ~1 kcal mol^{−1} higher. The scatter among different systems in the same phase is greater than the difference between the gas phase and solution phase. Given the quality of the barrier height data in both phases, there is no significant difference that can be seen in the magnitude of the steric effect between the two phases. The solvation energies of the corresponding transition states are, similarly, not much different, despite the very different sizes. This observation is consistent with IPCM and CPCM calculations, both of which show weak size dependence of the transition states in the β-series. The results agree with previous CPCM and QM/MM calculations comparing *tert*-butyl and methyl substitution.¹⁶

Solvation Energies. PCM was used to directly study the solvation energies of the S_N2 transition states. To test the performance of PCM on alkyl substitutions, solvation energies of alkyl-substituted carboxylates and alkoxides were calculated with IPCM and CPCM, Table 4. Both models predict that smaller anions are always solvated better. For example, when comparing CH₃COO[−] to (CH₃)₃CCOO[−], IPCM and CPCM predict that the solvation energy of CH₃COO[−] is ~2 and ~5 kcal mol^{−1} higher, respectively, Table 4. The experimental solvation energies, though not directly available, can be derived from their acidities, assuming no contribution from the neutrals (eq 7): acetic acid, CH₃COOH, is ~4 kcal mol^{−1} less acidic than pivalic acid, (CH₃)₃CCOOH, in the gas phase,⁶³ whereas their acidities in water are essentially the same, indicating ~4 kcal mol^{−1} difference in solvation energy of the corresponding carboxylates. Similar effects can be found for propionic acid, CH₃CH₂COOH, and isobutyric acid, (CH₃)₂CHCOOH. Both IPCM and CPCM models estimate the solvation energies of the carboxylates reasonably well. The alkoxide series is similar with even stronger negative size dependence. Each additional methyl group lowers the solvation energy by 2–3 kcal mol^{−1}, also consistent with the relative acidity differences from the gas phase to solution.

The origin of such negative size dependence of solvation energy is mostly a shielding effect, because the increasing substitution simply prevents the surrounding media from approaching the charge center. This problem has previously been

(59) Hirao, K.; Kebarle, P. *Can. J. Chem.* **1989**, *67*, 1261–1267.

(60) Streitwieser, A.; Choy, G. S.-C.; Abu-Hasanayn, F. *J. Am. Chem. Soc.* **1997**, *119*, 5013–5019.

(61) Mohamed, A. A.; Jensen, F. J. *Phys. Chem. A* **2001**, *105*, 3259–3268.

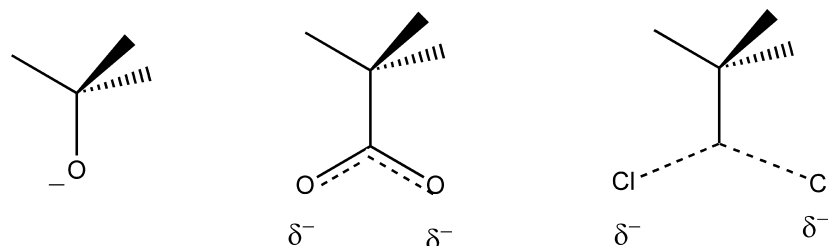
(62) Blavins, J.; Cooper, D.; Karadakov, P. *J. Phys. Chem. A* **2004**, *108*, 914–920.

(63) NIST Webbook <http://webbook.nist.gov>.

Table 9. Steric Effects in Solution and in the Gas Phase, Relative to Methyl

	$\Delta\Delta H^\ddagger$ (kcal mol ⁻¹) in solution (acetone)						$\Delta\Delta E$ (kcal mol ⁻¹) in the gas phase ^a		
	Br ⁻ RCH ₂ Br	Cl ⁻ RCH ₂ Br	Cl ⁻ RCH ₂ Br ^b	I ⁻ RCH ₂ Br	Cl ⁻ RCH ₂ I	Br ⁻ RCH ₂ I	Cl ⁻ RCH(CN)Cl ^c	Cl ⁻ RCH(CN)Cl ^d	Cl ⁻ RCH ₂ Cl ^d
methyl	0	0	0	0	0	0	0	0	0
ethyl	-0.1	0.3	-1.2	0.5	0.1	0.6	-0.2	-1.1	-1.2
isopropyl	1.6	1.4	0.3	1.1	1.0	0.2	1.0	1.0	0.3
<i>tert</i> -butyl	4.0	3.8	7.0	5.0	4.8		2.1	6.4	5.8

^a ΔE is defined as the energy difference between the transition state and reactants. ^b Reactions in this column are performed in dimethylformamide with Et₄N⁺ as the counterion. All others are in acetone with lithium cation. ^c Experimental barrier heights. ^d CBS-QB3 barrier heights.

**Figure 6.** Schematic of the alkoxides (RO⁻) and carboxylates (RCOO⁻) and the S_N2 transition states (Cl-RCH₂-Cl⁻).

addressed by Hawkins, Truhlar, and Cramer, who treated the individual atoms as if they had an effective Born radius which compensates for their screening by other atoms in the molecule.³² Polarization effects may also contribute a little, since alkyl groups usually facilitate charge distribution, and the more dispersed charge is less solvated.

The agreement between the PCM models and experiments is encouraging and the calculations are extended to the S_N2 transition states to estimate their solvation energies. Very weak size dependence, however, is found in the whole β -series by both CPCM and IPCM models, Table 4. Specifically, a very small difference between methyl and *tert*-butyl is observed and the order is even opposite.¹⁶ We conclude that no significant differential solvation is observed in the whole β -series between the transition states with different size, and therefore solvation does not affect the steric hindrance in solution very much in this system, just as our experimental data suggest.

The size independence of the solvation energies of these transition states appears to be inconsistent with the shielding model. Given the physical nature of the shielding effect and similar geometries among the systems, Figure 6, the solvation energy lowering effect from shielding in larger transition states must exist. Since the overall solvation energies appear to be about the same, regardless of size, there must be other factor(s) compensating. We propose it to be a result of geometric perturbations introduced by the additional methyl groups. B3LYP/CBSB7 predicts a gradually extended transition state with increasing β -methyl substitution; the C-Cl bond length increases 0.02–0.04 Å with every additional methyl group.

To investigate the substitution effect on solvation without accompanying geometric perturbations, the solvation energies of different alkyl substitutions were calculated with the geometry of the reaction center fixed. For example, the methyl, ethyl, isopropyl, and *tert*-butyl transition states are reoptimized with the two chlorides, and the reaction center carbon frozen at the configuration of the methyl transition state geometry. Three nonredundant coordinates, the two C-Cl bond lengths and the Cl-C-Cl angle, are frozen. CPCM solvation energies of such four transition states are -55.8, -55.3, -54.6, and -52.9 kcal mol⁻¹, respectively, listed as the first column in Table 5. The size dependence is immediately obvious, just as in the alkoxide series and the carboxylate series. When comparing methyl and

tert-butyl, one finds a 2–3 kcal mol⁻¹ difference in solvation energy, similar to the case of carboxylates listed in Table 4. We believe this is mostly due to the blocking of surrounding media by the extra methyl group, or the shielding effect. CPCM shows that a larger transition state would be poorly solvated if the geometry of the reaction center were unperturbed. The same series calculated at the other three configurations, originally optimized for ethyl, isopropyl, and *tert*-butyl, follow the same trend with a few exceptions.⁶⁴

With the four different alkyl substitutions, methyl through *tert*-butyl, optimized at the four configurations, a 4 × 4 matrix is obtained, as shown in Table 5. Top-to-bottom comparison represents the changes introduced by attaching an additional methyl group without perturbing its geometry. Alternatively, left-to-right comparison across the table shows what happens when the transition state extends without adding methyl groups. The solvation energies for the right entries are typically greater than the left entries, suggesting that transition states with longer C-Cl bonds are solvated better. The negative charge is less likely to be distributed to the central carbon because of the longer C-Cl bonds. An extreme case, when the bonds are infinitely long, would have one full negative charge located on each of the two chlorines. (It can be also seen as an S_N1 transition state.)^{34,65} Such an ionic transition state with more charge concentrated on chlorides should be solvated better. This is supported by the strong correlation between the solvation energies in Table 5 and NPA atomic charges on the chloride atoms in Table 6. More extended structures usually have more charge located on the chloride atoms and higher solvation energies as well.⁶⁴ Another contributing factor may be purely geometric, simply because the chloride atoms are further extended into the surrounding media and therefore interact more strongly with the surroundings. Thus, adding a methyl group will introduce a shielding effect but at the same time extend the transition state and increase its ionic character. Shielding lowers the solvation energy, and extension raises it. The two

(64) There are several exceptions to the general trends we have discussed; most involve isopropyl. The isopropyl transition state is asymmetric, with the two methyl groups pointing to one chloride, which is pushed away further than the other chloride. It may not be a good intermediate between methyl and *tert*-butyl.

(65) Kormos, B. L.; Cramer, C. J. *J. Org. Chem.* **2003**, *68*, 6375–6386.

compensating factors result in the weak size dependence of the solvation energy observed experimentally. Thus, solvation does not seem to contribute very much to the solution steric effect in the β -series. The general trend is the same by either CPCM or IPCM models and in different solvents.⁶⁴ More data are listed in Supporting Information.

Although the separation of the ionic solvation effect and shielding effect is not completely physical, this separation/simplification is a useful one. In this context, the shielding effect is always negative (making the steric effect in solution apparently greater) and the ionic solvation effect is always positive (making the steric effect in solution apparently weaker). The strengths of the both effects depend on the distance between the substituent and the reaction center: the shorter the distance, the stronger the effects are. However, the ionic solvation effect, which is an indirect result of the geometric changes, is more sensitive to the distance. On the other hand, the shielding effect, which is electrostatic (ion-induced dipole) in nature, works at much longer range. We believe that the cancellation between the two effects in the β -series is fortuitous. It is related to the intermediate distance between the substituent and the reaction center (two chemical bonds away). Consequently, we predict that the ionic solvation effect will dominate in the α -series because the substituent is closer to the reaction center (one chemical bond away). Several early gas-phase studies observed that the steric effect in the α -series is in fact greater than in solvent.^{20–23,57} On the other hand, if the substituent is far away from the reaction center, the ionic solvation effect becomes much weaker and the shielding effect becomes relatively more important. We have recently reported such a system where the substituent was varied on the nucleophile (three chemical bonds away from the reaction center),^{66,67} but in that system, the differential solvation is mostly on the reactant rather than the

transition state. Therefore the shielding effect would make the steric effect apparently stronger, and indeed that was what we have observed experimentally.

Summary

In summary, we have studied the steric effect in the β -series of the gas-phase S_N2 reactions of chloride with chloronitriles. The systems were proven to be good models for the parent reactions of chloride with alkyl chlorides, which are too slow to measure experimentally. The cyano-substituted systems were investigated computationally as well, together with the parent systems. Similar steric hindrance effects were observed in both series. When comparing the gas-phase results with solution, we found no significant difference in the magnitude of the steric effect between the two phases, which is consistent with solvation energy calculations by two polarizable continuum models. Overall, the size dependence of solvation is very weak in the S_N2 transition states, in contrast to other simple ionic systems such as alkoxides and carboxylates. Polarizable continuum model calculations with fixed geometry suggest that this effect may be attributed to the compensation between the negative shielding effect and the positive ionic solvation effect; the latter is caused by geometry changes with additional methyl groups. Comparable results were obtained in a recently submitted theoretical study.³⁴

Acknowledgment. We are grateful to the National Science Foundation (J.I.B., S.L.C., K.N.H., W.L.J.), Stanford University Stanford Graduate Fellowship (X.C.), the Australian-American Fulbright Commission (E.H.K.), and the UCLA IDRE for computer resources (K.N.H.). We thank Professor D. Truhlar for sharing results with us and for helpful suggestions.

Supporting Information Available: Geometries and energies of the S_N2 transition states. This material is available free of charge via the Internet at <http://pubs.acs.org>.

JA9053459

(66) Chen, X.; Brauman, J. I. *J. Am. Chem. Soc.* **2008**, *130*, 15038–15046.
(67) Chen, X.; Walthall, D. A.; Brauman, J. I. *J. Am. Chem. Soc.* **2004**, *126*, 12614–12620.